PLANT SCIENCE

Defining the developmental program leading to meiosis in maize

Brad Nelms* **and Virginia Walbot***

In multicellular organisms, the entry into meiosis is a complex process characterized by increasing meiotic specialization. Using single-cell RNA sequencing, we reconstructed the developmental program into maize male meiosis. A smooth continuum of expression stages before meiosis was followed by a two-step transcriptome reorganization in leptotene, during which 26.7% of transcripts changed in abundance by twofold or more. Analysis of cell-cycle gene expression indicated that nearly all pregerminal cells proliferate, eliminating a stem-cell model to generate meiotic cells. Mutants defective in somatic differentiation or meiotic commitment expressed transcripts normally present in early meiosis after a delay; thus, the germinal transcriptional program is cell autonomous and can proceed despite meiotic failure.

Meiosis is key to the life cycle of sexually reproducing organisms, halving chromosome number and generating new allele combinations through recombination. The mechanisms that regulate meiotic entry in plants are not well understood (*1*, *2*) but directly affect crop breeding and agricultural yield (*3*). In maize anthers, hypoxia triggers somatic cells to differentiate as archesporial cells (*1*), the first cell type in the meiotic lineage. After a ~3-day period of transit-amplifying mitotic divisions, archesporial cells cease mitosis, become pollen mother cells, and enter meiotic prophase. Cell morphology (*4*) and gene expression (*5*–*8*) change during premeiotic and early meiotic development, but the timing of these events and relationship to meiotic chromosome stages are unknown. Are there intermediate cellular stages with distinct gene expression profiles during premeiotic archesporial cell differentiation? Do large changes in expression signal the start of meiotic prophase?

We applied single-cell RNA sequencing (scRNA-seq) to characterize the developmental program leading to male meiosis in maize. We introduce a quantitative framework, "pseudotime velocity," to infer developmental transitions based on periods of relatively rapid gene expression change and apply this framework to identify cellular intermediates during germinal development. These results provide a roadmap for reconstructing plant developmental pathways with scRNA-seq.

scRNA-seq of premeiotic and early meiotic cells

Maize male germinal cells form within immature anthers, centrally located in each of four anther lobes (Fig. 1A). Anthers expand reproducibly during early development; consequently, anther length is a reliable proxy for both developmental stage and organ age (*4*). Germinal development is regular but asynchronous before meiosis, after which all meiocytes in an anther progress through meiosis in unison (*4*). We established methods to isolate single premeiotic and meiotic cells from maize anthers for scRNA-seq (Fig. 1B). Cells in the germinal lineage are two to four times larger in diameter than all other anther cells (*4*), permitting identification after tissue dissociation (Fig. 1B and fig. S1). To minimize expression changes during sample handling, isolated cells were obtained and frozen within 1 to 2 hours of plant harvest. After cell lysis, samples were divided into two tubes and processed independently as split-cell technical replicates.

Using this protocol, we isolated germinal cells from 24 plants, covering a week of development from the day after archesporial cell specification to early zygotene of meiotic prophase I (fig. S2 and table S1). High-quality reads were obtained from 144 cells (fig. S3), with a mean of 101,245 transcripts detected per cell. Technical replicates produced reproducible transcript counts [median coefficient of determination r^2 = 0.92] (Fig. 1C and fig. S4). The majority (64.2%) of expression

Department of Biology, Stanford University, Stanford, CA 94305, USA.
*Corresponding author. Email: bnelms.research@gmail.com (B.N.); walbot@stanford.edu (V.W.)

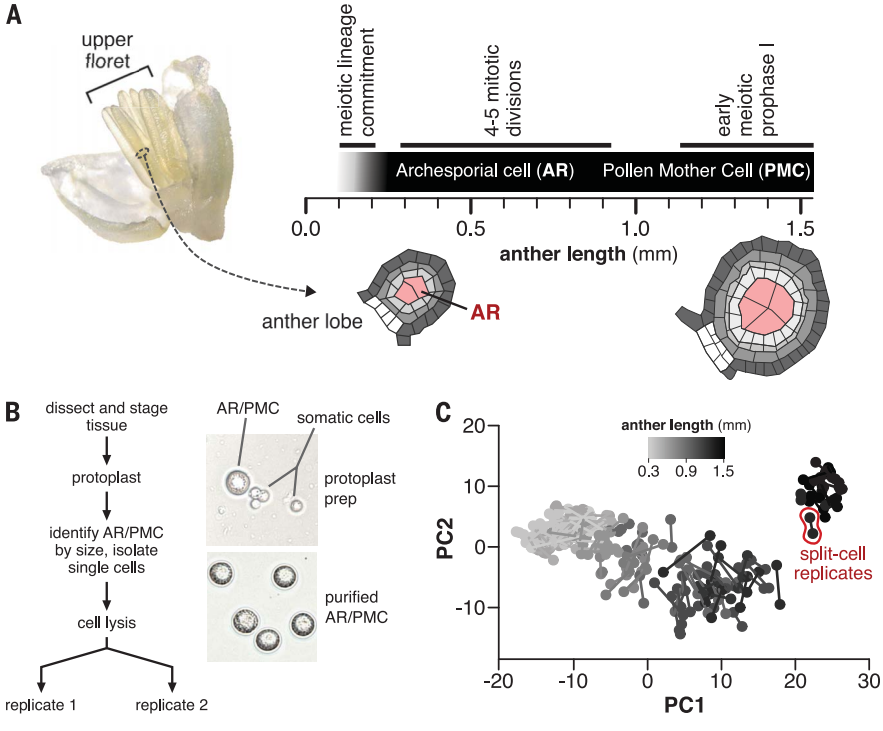

Fig. 1. scRNA-seq of premeiotic and early meiotic cells. (**A**) Schematic of early maize anther development. Single cells were isolated from 0.3- to 1.5-mm anthers. (**B**) Flow chart of cell isolation and single-cell library preparation. Germinal cells were identified by their large size; technical replicates were prepared by splitting single-cell contents immediately after lysis. (**C**) Principal component analysis shows that major axes of variation closely reproduce tissue stage. Replicate samples were considered independently and then connected with a line for visualization. AR, archesporial cell; PMC, pollen mother cell; PC, principal component.

Downloaded from http://science.sciencemag.org/ on May 20, 2021

variance was explained by tissue stage (fig. S5); by contrast, only 1% of variance could be attributed to cell isolation time (fig. S5), suggesting that expression changes during tissue dissociation were small relative to the preexisting biological variability. A set of 375 genes (2.1% of the 12,902 "expressed" genes) (table S2) formed clusters indicative of cell-cycle stage (fig. S6); to focus on developmental events, these genes were excluded unless specified otherwise.

Dynamics of early germinal cell differentiation

To identify intermediate stages from our data, we initially applied clustering to group cells with similar gene expression patterns (fig. S7A). However, clustering removed information about developmental dynamics: Some clusters had sharper boundaries than others, and many had internal structure not captured by discrete groupings. Consequently, we tested a continuous framework to assess cell-to-cell variation and developed a statistic, pseudotime velocity, to quantify the rate of gene expression change over time.

First, we applied dimensionality reduction to determine pseudotime (*9*, *10*), a single variable that captured much of the relative gene expression difference between cells as well as their inferred developmental order (Fig. 2A). Pseudotime estimates were reproducible between split-cell technical replicates (r^2 = 0.97) (Fig. 2A, inset). Then, we ordered samples by increasing pseudotime and calculated pseudotime velocity as the linear slope in pseudotime between adjacent ordered samples within a rolling window (Fig. 2B and fig. S8). Pseudotime velocity showed a consistent rate of expression change initially, followed by three peaks with significantly greater velocity than the median (Fig. 2C). Peaks agreed with cluster boundaries defined by the consensus of eight single-cell clustering methods (fig. S7), but pseudotime velocity also preserved details obscured by clustering. For example, the height of the velocity peaks provided a means to quantify the relative magnitude of each expression shift. Second, the velocity remained under twice the median during the first half of the time course (Fig. 2C), suggesting a period of continuous expression change not captured by clustering. To investigate the features leading to differences in velocity, we identified differentially expressed genes (3046 genes) (table S3) and visualized their expression in a heatmap (Fig. 2D). The heatmap reproduced features quantified by pseudotime velocity: There were first smooth, continuous changes in gene expression followed by steplike discrete shifts. Thus, we found evidence for periods of continuous and discrete differentiation in this single lineage.

To connect pseudotime velocity to the established developmental progression, we grouped cells by pseudotime (Fig. 2C, colored boxes) and then evaluated the anther lengths from which they were isolated. The continuous period of gene expression (Fig. 2C, blue and gray boxes) contained cells from ≤1.1-mm anthers—the archesporial and early pollen mother cell stages (*4*). There were no sharp changes in expression to indicate the point when archesporial cells ceased their mitotic divisions and transitioned into pollen mother cells. Gene expression was not static during archesporial development; one-third of all pseudotime change occurred during this period. Nonetheless, expression in the archesporial population was a continuum without sudden shifts reflecting rapid differentiation events.

After the second pseudotime velocity peak, all cells were from ≥1.3-mm anthers. On average, meiotic prophase I begins in 1.2-mm anthers (fig. S9), indicating that the final two peaks occurred during early meiotic prophase. We subsequently refer to these expression shifts as "prophase expression transition 1" (Pr1) and "prophase expression transition 2" (Pr2). We estimate that these transitions each occurred in under 10 hours (supplementary materials).

Gene expression shifts during meiotic prophase

The identification of two transcriptional shifts during prophase I led us to ask how these expression changes related to meiotic chromosome cytology. We selected five marker genes from the scRNA-seq data to stage Pr1 and Pr2 (Fig. 3A): two genes down-regulated during both Pr1 and Pr2 (*Ago18a* and *Rpl38e*), two up-regulated during Pr1 (*Rmf* and *C3h3*), and one up-regulated during Pr2 (*Trps8*). Then, we compared gene expression

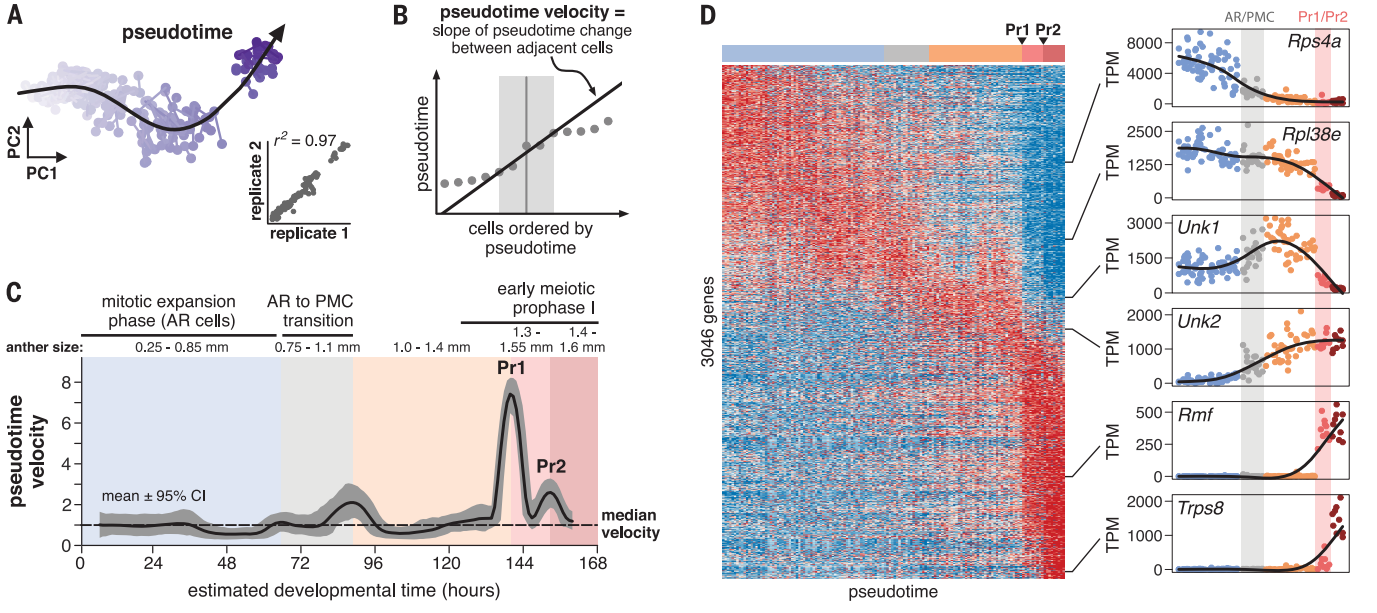

Fig. 2. Germinal differentiation is characterized by both gradual and discrete cell-state transitions. (**A**) Pseudotime was calculated by fitting a principal curve to the first 10 principal components. (Inset) Pseudotime estimates were reproducible between technical replicates. (**B**) Pseudotime velocity was calculated as the linear slope in pseudotime between ordered samples within a rolling 10-sample window; results were consistent with window sizes from 2 to 15 samples (fig. S8). (**C**) Pseudotime velocity as a function of estimated developmental time. Units are relative to median velocity, and the gray outline denotes the 95% CI. Anther size was determined as the range of anthers from which cells within each colored box were isolated. Pr1, prophase expression transition 1; Pr2, prophase expression transition 2. (**D**) Heatmap of gene expression for all differentially regulated genes. Color ranges from blue (minimum) to red (maximum transcripts per million) for each gene. AR, archesporial cell; PMC, pollen mother cell. TPM, transcripts per million; *Unk1*, *Unknown gene 1* (Zm00001d027037); *Unk2*, *Unknown gene 2* (Zm00001d013377).

Downloaded from http://science.sciencemag.org/ on May 20, 2021

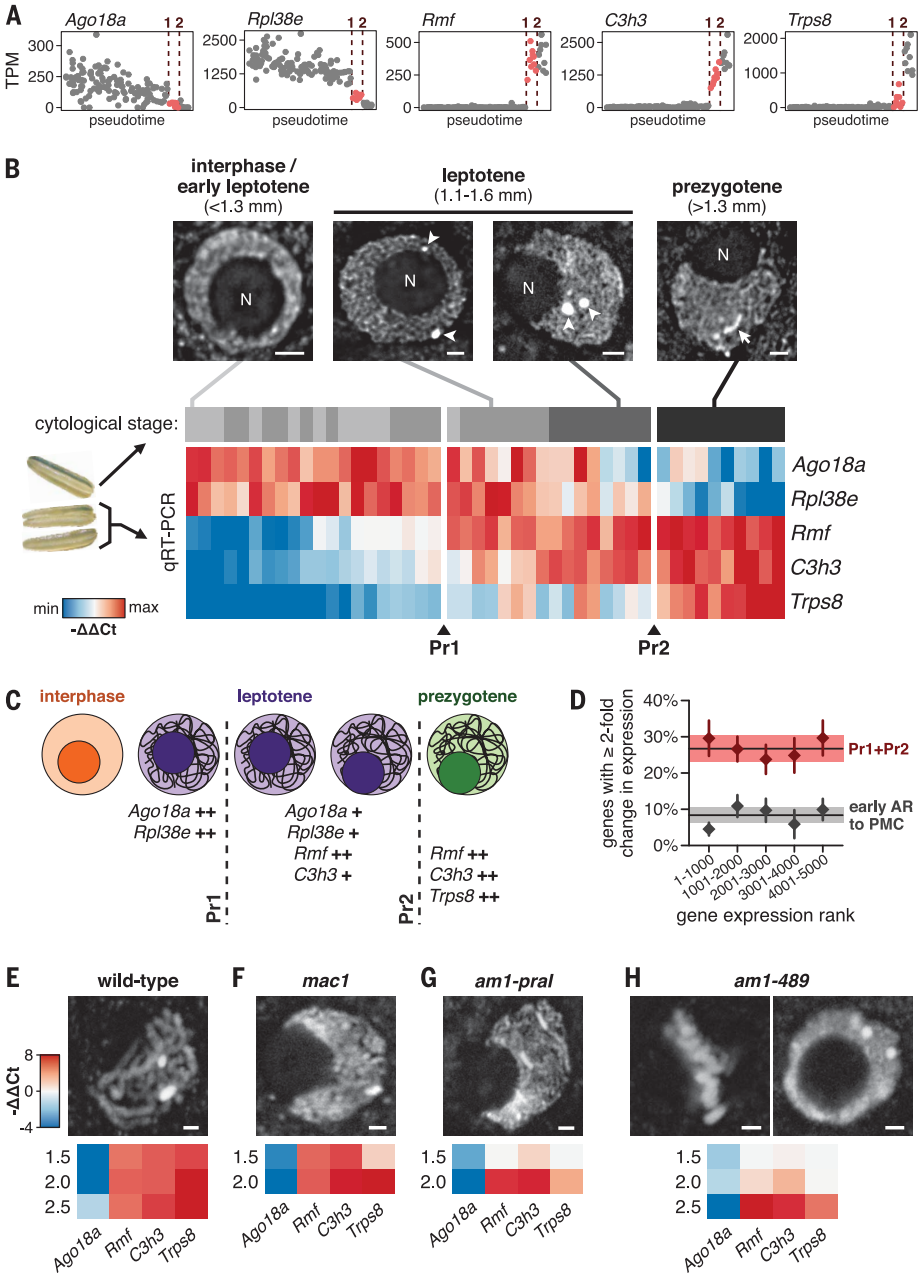

Fig. 3. Transcriptome reorganization during leptotene. (**A**) Marker genes for Pr1 and Pr2. Cells between Pr1 and Pr2 in development are colored red. (**B**) Alignment of gene expression states to cytology in 1.1- to 1.6-mm anthers. (Top) Hoechst staining of meiotic nuclei. Anthers were classified into four cytological stages based on the presence or absence of condensed chromosomes throughout the nuclear volume, the location of the nucleolus at the center or periphery of the nucleus, and spherical or elongated knob morphology. N, nucleolus; arrowhead, spherical knobs; arrow, elongated knob. Scale bar, 2 μm. (Bottom) Expression of marker genes in isolated meiocytes. Cytology and expression data from each column were obtained from the same floret. Cytological scoring was performed blinded to sample identity. (**C**) Illustration of relationship between cytology and expression during early leptotene. "++" indicates a marker gene is at its maximum expression level; "+" indicates a marker gene is expressed above 20% of its maximum level. (**D**) Estimated percentage of genes with a ≥2-fold change in expression (i) during Pr1 and Pr2 or (ii) between early archesporial cells and pollen mother cells. Black horizontal lines and shaded area indicate the mean ± 95% CI for the estimated percentage of genes that change ≥2-fold when calculated with the top 5000 expressed genes; diamonds indicate estimates for subsets of these genes grouped by overall expression level. (**E** to **H**) (Top) Germinal cell cytology in 2-mm anthers. Scale bar, 2 μm. (Bottom) Marker gene expression relative to 1-mm anthers. *Rpl38e* was not considered for this analysis because it is broadly expressed in somatic cells; all other marker genes are selectively expressed in meiocytes (*5*).

to chromosome cytology in 1.1- to 1.6-mm anthers isolated from 46 individual florets. One of three synchronously developing anthers from each floret was fixed for cytology, whereas meiotic cells were harvested from the other two for quantitative polymerase chain reaction (qPCR).

Marker gene expression by means of qPCR showed changes consistent with the scRNA-seq data (Fig. 3B) and was correlated with the cytological progression. Pr1 markers (*Rmf* and *C3h3*) were expressed at low levels during premeiotic interphase and early leptotene, up-regulated in 7 of 17 florets (41%) in the "leptotene with a central nucleolus" stage, and strongly expressed at all later cytological stages; we conclude that the Pr1 transition occurred within the leptotene with a central nucleolus stage. The Pr2 marker gene *Trps8* was up-regulated in all florets in prezygotene (*11*) but not earlier, indicating that Pr2 occurred at the entry into prezygotene. These results show that cytology and gene expression provide complementary views of cell state and do not perfectly overlap (Fig. 3C).

The combined expression change during Pr1 and Pr2 included a twofold or greater shift in transcript abundance for 1335 of the top 5000 most-expressed genes [26.7%; 95% confidence interval (CI) = 23.1%, 30.3%] (Fig. 3D). By comparison, we observed a twofold change in only 8.4% of transcripts between the earliest archesporial cells and the start of meiotic prophase I (CI = 6.2%, 10.5%)—a 5-day period that included the mitosis-to-meiosis transition. These findings were consistent for genes at different thresholds of overall abundance (Fig. 3D) and were not sensitive to normalization (fig. S10).

Do the Pr1 or Pr2 transitions require input from somatic cells or meiotic chromosomal reorganization? To answer this, we determined whether Pr1 and Pr2 marker genes were expressed in mutants defective in somatic differentiation or meiotic progression. First, we examined *multiple archesporial cells 1* (*mac1*), a mutant that lacks differentiated somatic cells around the meiocytes and yet the germinal precursors enter meiosis (*12*). We observed normal marker expression in *mac1* other than a delayed up-regulation of the Pr2 marker *Trps8* (Fig. 3F), indicating that the regulation of these genes does not require signaling from the adjacent soma. We next examined two alleles of *ameiotic1* (*am1*): *am1-praI* and *am1-489*. The *am1-praI* allele enters meiotic prophase but stalls in the prezygotene stage (*13*). We considered the possibility that *am1-praI* might have transcriptome defects during leptotene that precede the later chromosomal arrest; however, all Pr1 and Pr2 markers were expressed in *am1-praI* meiocytes after a delay (Fig. 3G). Last, we examined *am1-489*, a mutant allele that results in asynchronous mitosis instead of meiosis in germinal cells (*13*). Marker expression was abnormal in *am1-489* through the 2-mm anther stage (late prophase I in normal anthers); however, in 2.5-mm anthers (tetrad stage in normal meiosis), the markers reached levels comparable with that of wild type (Fig. 3H). Chromosome morphology remained abnormal in 2.5-mm

Downloaded from http://science.sciencemag.org/ on May 20, 2021

am1-489 anthers (fig. S11); therefore, the expression of early prophase marker genes was decoupled from meiotic chromosome morphology in this mutant. We conclude that the Pr1 and Pr2 transitions are cell autonomous and can proceed in the absence of normal meiotic progression.

Coordination between nuclear and cytosolic events

To determine which genes were regulated during germinal differentiation, we grouped all differentially expressed genes by unsupervised clustering and asked which pathways were enriched in each (Fig. 4A). Genes required for core meiotic functions (table S4) (*2*), such as recombination and synapsis, were enriched in both up-regulated clusters ($P = 1.9 \times 10^{-2}$ and 2.9×10^{-8} for clusters 5 and 6, respectively; Fisher's exact test). There was a loose association between when each meiotic gene was up-regulated and the established timing of the encoded protein function (Fig. 4B): Genes encoding proteins that act before meiotic prophase, such as the cohesin subunit *Absence of first division1* (*Afd1*), were up-regulated before later-acting genes, such as *Synaptonemal complex protein ZIPPER1* (*Zyp1*). There was also an enrichment for genes differentially expressed in meiotic cells relative to the surrounding soma (*5*) in clusters 4, 5, and 6 (Fig. 4C); however, spatial expression in meiocytes and temporal expression during meiosis did not always align. For instance, *Ago18a* was down-regulated during leptotene (Fig. 3), even though it is expressed selectively in meiocytes (*5*).

Pathway analysis by use of AgriGO (*14*) highlighted changes in metabolism and cell biology during germinal differentiation (Fig. 4A and table S5). There was a shift in the proportion of transcripts annotated to specific cellular organelles (fig. S12), including an enrichment for genes linked to the membrane-bound organelles mitochondria, endoplasmic reticulum, and Golgi in clusters 5 and 6. In parallel, there was a reduction in transcripts encoding the protein translation machinery. Genes associated with the Gene Ontology (GO) term "translation" composed 20 and 30% of the two major down-regulated gene clusters (clusters 2 and 3, respectively) (Fig. 4D). These encode proteins involved in ribosome biogenesis, translation elongation, and tRNA metabolism, as well as structural subunits of cytosolic ribosomes. The total expression of transcripts encoding ribosomal proteins decreased by 326% (Fig. 4E), with the sharpest decline (243%) during early prophase. These findings were consistent with established cellular remodeling during meiotic prophase in plants, such as an increase in the number and volume of mitochondria (*15*) and other heterogeneous membrane structures (*16*) and a 1000% decrease in the number of cytosolic ribosomes (*16*). Thus, meiotic expression reflects regulation of transcripts linked to both chromosomal remodeling and differentiation of the meiotic cytoplasm.

Cell-cycle regulation in mitosis and meiosis

The asynchronous mitotic divisions of archesporial cells complicate efforts to understand gene regulation during this period by using bulk tissue. Single-cell methods can deconvolve this heterogeneity. We identified gene clusters within the dataset associated with specific cell-cycle phases (Fig. 5A, fig. S6, and table S2), and from this, we inferred the cell-cycle phase of each cell (Fig. 5B). The proportion of cells predicted to be in S phase at a given anther length (Fig. 5C) was in agreement with prior estimates (*4*), but the single-cell data provided a more complete picture because many cell-cycle phases were identifiable simultaneously. Previously, it was unclear whether most archesporial cells contribute to mitotic divisions or whether a fraction of cells serve as a stem-cell population that divides asymmetrically to populate the anther lobe (*1*, *4*). We can now conclude that the majority of cells contribute because 92.5% were in the cell cycle during the peak mitotic stage (0.5-mm anthers).

Are there "cell cycle–regulated" genes specific to mitosis or meiosis? During mitotic proliferation before meiotic prophase I, we found a cyclical pattern of genes associated with specific cell-cycle phases (Fig. 5B). Meiotic cells, by contrast, coexpressed genes associated with multiple mitotic cell-cycle phases (Fig. 5B and fig. S6). For example, meiocytes expressed several histone subunits (expressed in archesporial cell S phase) together with microtubule-binding proteins (expressed in archesporial cell G2/M phase) and expressed combinations of cyclins and cyclin-dependent kinases not observed in the archesporial population. These results highlight features that distinguish meiotic prophase I and mitotic cell cycles in the predecessor cell population.

We queried our data to identify developmentally regulated genes during the archesporial cell stage (cells from anthers ≤1 mm in length) by calculating how the expression of each gene was correlated with (i) pseudotime and (ii) the most similar cell-cycle cluster. This analysis separated genes that change in expression during

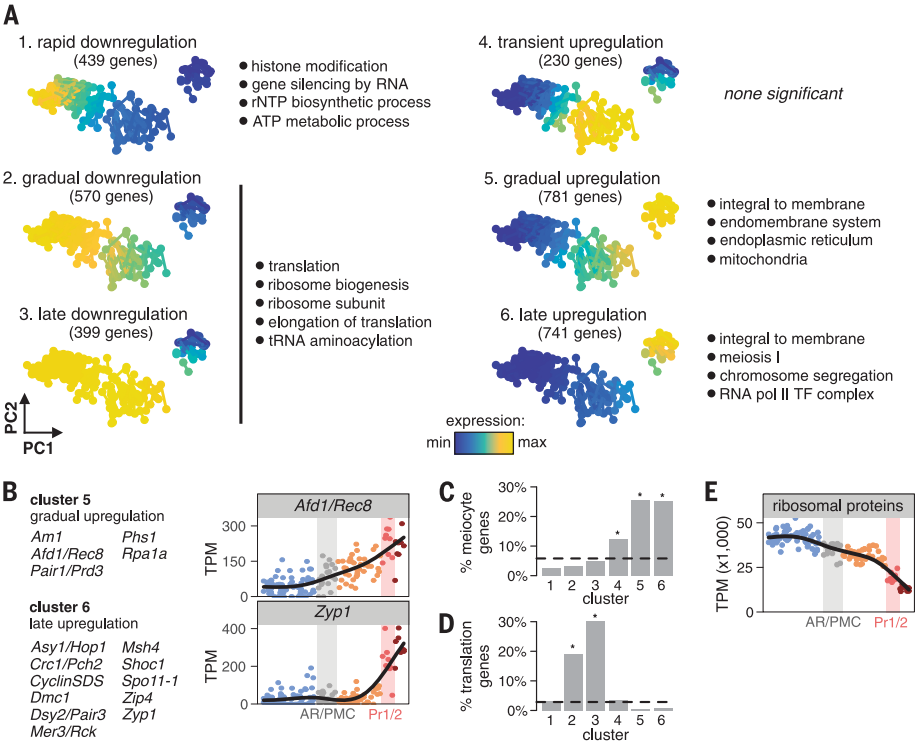

Fig. 4. A global view of transcriptional regulation during germinal differentiation. (**A**) Principal component plots showing mean expression in six coregulated gene clusters. Bullet points are enriched GO terms. (**B**) Expression of genes with established roles in meiotic prophase I (*2*). (**C** and **D**) Percentage of genes in each cluster (C) more strongly expressed in meiocytes than the surrounding soma (*5*) or (D) annotated with the GO term "translation." Dotted line indicates expected percent of genes in each cluster if genes were randomly sampled. Asterisk indicates significant enrichment relative to the genomic background; $P < 0.05$, Fisher's exact test. (**E**) Cumulative expression of transcripts encoding protein subunits of the cytosolic ribosome.

Downloaded from http://science.sciencemag.org/ on May 20, 2021

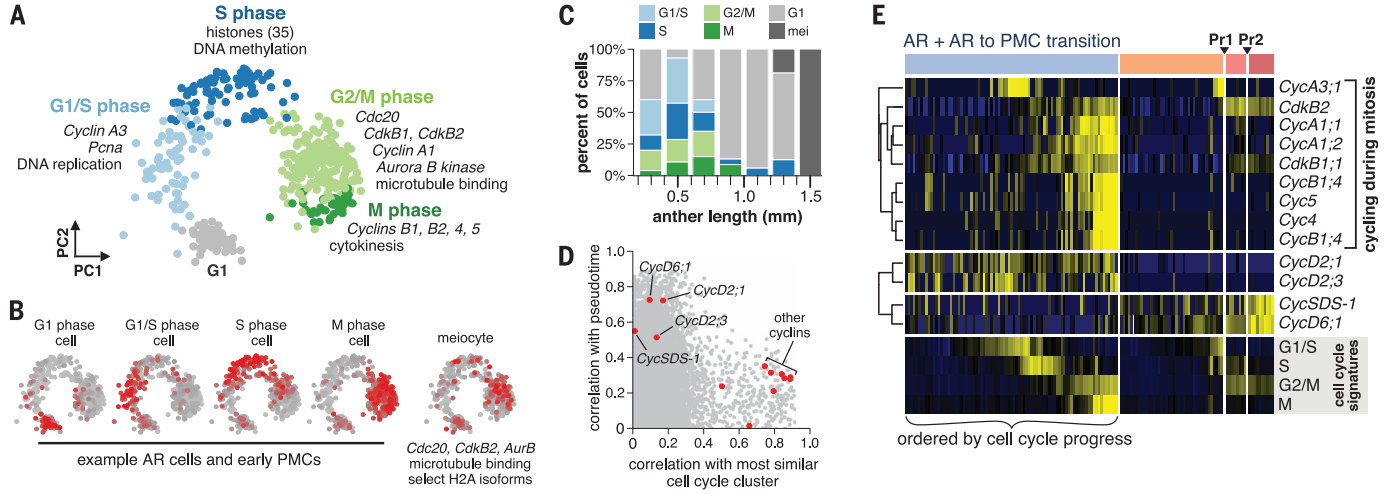

Fig. 5. Cell cycle–regulated gene expression in mitosis and meiosis. (**A**) Principal component plot of cell cycle–regulated genes. Each point (gene) colored according to its assigned cell-cycle cluster. (**B**) Expression of cell cycle–regulated genes in representative cells at different cell-cycle phases. (**C**) Estimated proportion of cells assigned to each cell-cycle phase. (**D**) Correlation of all genes with the most similar mitotic cell-cycle cluster and with pseudotime. Cyclins are highlighted in red. (**E**) Heatmap of gene expression for cyclins and cyclin-dependent kinases.

archesporial differentiation from cell cycle–regulated genes (Fig. 5D), a distinction that would have been impossible by using data from whole anthers (Fig. 5C and fig. S13). Nine cyclins were selectively expressed at specific cell-cycle phases (Fig. 5E), as expected given their role as key cell-cycle regulators. A subset, however, was not correlated with any cell-cycle phase but rather showed stage-dependent expression regulation. Two cyclins were up-regulated during leptotene, including *CycSDS-1*, one of two homologs of a regulator of meiotic prophase I in *Arabidopsis* (*17*). By contrast, *CycD2;1* and *CycD2;3* were constitutively expressed in mitotic archesporial cells and then down-regulated during the mitosis-to-meiosis transition.

Discussion

During the transit-amplifying divisions of archesporial cells and their cessation of mitosis, we found steady transcriptome changes without sudden shifts in expression. This was followed by a reorganization of the transcriptome in two sharp transitions. By comparing these transitions to chromosome cytology, we found that the first occurs within leptotene, whereas the second is at the boundary of prezygotene, a cytology stage in maize that occurs just before the onset of chromosome pairing (*11*). Intriguingly, a recent survey of mouse spermatogenesis also observed a jump in gene expression near the beginning of meiosis (*18*). Although the timing of this expression change relative to meiotic prophase stages was not determined, it may be analogous to the leptotene transcriptome reorganization defined here.

What is the reason for such a large shift in expression during early meiotic prophase? Our data suggest that the prophase expression transitions relate not only to nuclear events during prophase I but also to changes in cellular physiology. There was a loss of ribosomal transcripts and an increase in transcripts encoding components of membrane-bound organelles and mitochondria, which is consistent with established changes in the meiotic cytoplasm in plants (*15*, *16*). Meiotic cytoplasmic remodeling may be partially connected to the alternation of generations because meiosis is the bridge from the diploid to haploid stages of the life cycle. Animal oocytes carry mRNA stored for future, postzygotic translation (*19*), and one possibility is that some mRNAs synthesized during leptotene are translated post-meiotically in maize. Ribosome elimination during meiosis could be a mechanism to degrade long-lived messenger RNAs and proteins before the gametophytic stage (*16*), accelerating the switch to functions encoded by the haploid genome.

In contrast to animals, plants continue germinal development in mutants with defects in the somatic cell layers (*12*) or meiotic progression (*20*). In *mac1*, for example, somatic cells are abnormal in early-stage anthers (0.3 mm), yet the germinal cells reach meiosis before eventual organ failure (*12*). The resilience of the plant germinal program makes it possible to follow the downstream consequences of earlier defects and separate processes that are normally coordinated. We found that marker genes up-regulated during early meiotic prophase reached expression levels comparable with that of wild-type in *am1-489*, a mutant that undergoes mitosis instead of meiosis (*13*). Thus, at least part of the transcriptional reorganization that accompanies meiosis does not strictly require meiotic chromosomal progression. We propose that transcriptome regulation during meiosis connects the meiotic cell cycle to larger changes in cell physiology and differentiation during germinal development.

REFERENCES AND NOTES

1. T. Kelliher, R. L. Egger, H. Zhang, V. Walbot, *Front. Plant Sci.* **5**, 347 (2014).
2. R. Mercier, C. Mézard, E. Jenczewski, N. Macaisne, M. Grelon, *Annu. Rev. Plant Biol.* **66**, 297–327 (2015).
3. W. Crismani, C. Girard, R. Mercier, *J. Exp. Bot.* **64**, 55–65 (2013).
4. T. Kelliher, V. Walbot, *Dev. Biol.* **350**, 32–49 (2011).
5. S. Dukowic-Schulze *et al.*, *BMC Plant Biol.* **14**, 118 (2014).
6. H. Zhang *et al.*, *G3 (Bethesda)* **4**, 993–1010 (2014).
7. T. L. Yuan, W. J. Huang, J. He, D. Zhang, W. H. Tang, *Plant Physiol.* **176**, 1610–1626 (2018).
8. S. Dukowic-Schulze *et al.*, *J. Genet. Genomics* **41**, 139–152 (2014).
9. T. Hastie, W. Stuetzle, *J. Am. Stat. Assoc.* **84**, 502–516 (1989).
10. C. Trapnell *et al.*, *Nat. Biotechnol.* **32**, 381–386 (2014).
11. R. K. Dawe, J. W. Sedat, D. A. Agard, W. Z. Cande, *Cell* **76**, 901–912 (1994).
12. C.-J. R. Wang *et al.*, *Development* **139**, 2594–2603 (2012).
13. W. P. Pawlowski *et al.*, *Proc. Natl. Acad. Sci. U.S.A.* **106**, 3603–3608 (2009).
14. T. Tian *et al.*, *Nucleic Acids Res.* **45** (W1), W122–W129 (2017).
15. S. Lee, H. Warmke, *Am. J. Bot.* **66**, 141–148 (1979).
16. H. G. Dickinson, J. Heslop-Harrison, *Philos. Trans. R. Soc. London B Biol. Sci.* **277**, 327–342 (1977).
17. Y. Azumi *et al.*, *EMBO J.* **21**, 3081–3095 (2002).
18. C. D. Green *et al.*, *Dev. Cell* **46**, 651–667.e10 (2018).
19. J. D. Richter, P. Lasko, *Cold Spring Harb. Perspect. Biol.* **3**, a002758 (2011).
20. A. P. Caryl, G. H. Jones, F. C. Franklin, *J. Exp. Bot.* **54**, 25–38 (2003).

ACKNOWLEDGMENTS

We thank the Carnegie Institution Plant Biology Imaging Facility for use of the SP8 microscope; B. Meyers for valuable input; and M. Staller, R. Erdmann, and B. Marchant for critical reading of the manuscript. **Funding:** This work was supported by National Science Foundation awards 1649424 (to V.W.) and 1611975 (to B.N.). **Author contributions:** B.N. conducted experiments and analyzed data, with input from V.W.; B.N. and V.W. designed the study and wrote the manuscript. **Competing interests:** The authors declare no competing interests. **Data and materials availability:** Sequencing data are deposited to the Gene Expression Omnibus (accession no. GSE121039). All other data needed to evaluate the conclusions of this manuscript are present in the main text or supplementary materials.

SUPPLEMENTARY MATERIALS

www.sciencemag.org/content/364/6435/52/suppl/DC1
Materials and Methods
Figs S1 to S13
Tables S1 to S7
References (*21*–*35*)

6 October 2018; accepted 1 March 2019
10.1126/science.aav6428

Downloaded from http://science.sciencemag.org/ on May 20, 2021

Science

Defining the developmental program leading to meiosis in maize

Brad Nelms and Virginia Walbot

Science **364** (6435), 52-56.
DOI: 10.1126/science.aav6428

Following meiosis in maize

Plants do not set aside a germ-cell lineage from early development as animals do, but instead generate germ cells on demand. Nelms and Walbot, working in maize, took advantage of a size differential between somatic and developing germ cells in the anthers at the top of the maize plant to isolate individual germ cells during the meiotic progression to pollen development. They used single-cell RNA sequencing to study changes in the transcriptome through meiosis. These studies revealed increasing specialization as meiosis progressed, with a reorganization of the transcriptome in a transition during the leptotene stage of meiosis.

Science, this issue p. 52

ARTICLE TOOLS http://science.sciencemag.org/content/364/6435/52

SUPPLEMENTARY MATERIALS http://science.sciencemag.org/content/suppl/2019/04/03/364.6435.52.DC1

REFERENCES This article cites 33 articles, 6 of which you can access for free
http://science.sciencemag.org/content/364/6435/52#BIBL

PERMISSIONS http://www.sciencemag.org/help/reprints-and-permissions

Use of this article is subject to the Terms of Service

Science (print ISSN 0036-8075; online ISSN 1095-9203) is published by the American Association for the Advancement of Science, 1200 New York Avenue NW, Washington, DC 20005. The title *Science* is a registered trademark of AAAS.

Copyright © 2019 The Authors, some rights reserved; exclusive licensee American Association for the Advancement of Science. No claim to original U.S. Government Works

Downloaded from http://science.sciencemag.org/ on May 20, 2021